Supplementary Information

A Theoretical Study of NH₂ Radical Reactions with Propane and Its Kinetic Implications in NH₃-Propane Blends Oxidation

Binod Raj Giri[1, *], Krishna Prasad. Shrestha[2, *], Tam V.-T. Mai[3,4], Sushant Giri[1], Mohammad Adil[1], R. Thirumaleswara Naik[1,5], Fabian Mauss[6], and Lam K. Huynh[7,8, *]

[1]*King Abdullah University of Science and Technology (KAUST), Physical Science and Engineering Division, Clean Combustion Research Center, Thuwal 23955-6900, Kingdom of Saudi Arabia*

[2] *Physics and Chemistry of Materials, Theoretical Division, Los Alamos National Laboratory, Los Alamos, New Mexico 87545, United States*

[3]*Institute of Fundamental and Applied Sciences, Duy Tan University, 06 Tran Nhat Duat, Tan Dinh Ward, District 1, Ho Chi Minh City, Vietnam.*

[4]*Faculty of Natural Sciences, Duy Tan University, Da Nang City, Vietnam*

[5]*Department of Mechanical Engineering, Indian Institute of Science, Bangalore, India*

[6]*Thermodynamics and Thermal Process Engineering, Brandenburg University of Technology, Siemens-Halske-Ring 8, 03046 Cottbus, Germany*

[7]*International University, Quarter 6, Linh Trung Ward, Thu Duc City, Ho Chi Minh City, Vietnam.*

[8]*Vietnam National University, Ho Chi Minh City, Vietnam*

*Corresponding authors: Binod Raj Giri (binod.giri@kaust.edu.sa)
Krishna Prasad Shrestha (sthakrish@gmail.com)
Lam K. Huynh (hklam@hcmiu.edu.vn)

Contents

Table S1: Calculated M06-2X/aug-cc-pVTZ harmonic vibrational wavenumbers and rotational constants of the stationary points for the $NH_2 + C_3H_8$ reaction. Imaginary wavenumbers are denoted by i.

Species	Rotational Constants / GHz	Wavenumbers / cm^{-1}		
NH_2	712.90702 387.56034 251.07013	1529.8351	3402.7529	3491.2944
NH_3	299.84485 299.82821 189.10734	1030.7854 3508.1781	1658.8781 3632.5664	1659.6292 3634.1800
C_3H_8	29.48604 8.53912 7.54269	**217.1730** 751.4273 934.0276 1215.4603 1406.6894 1494.8185 1516.2901 3060.3544 3127.0070	**277.8019** 892.1307 1078.4783 1318.3209 1421.5207 1499.4468 3054.5024 3084.4746 3130.4892	371.8257 913.0741 1182.0993 1367.0798 1493.0354 1511.2097 3055.1605 3116.5587 3132.2473
PC1	12.52610 2.39088 2.10994	36.5392 100.0770 218.0240 554.0530 912.2017 1106.0554 1332.9553 1492.1647 1655.4973 3060.1393 3135.5623 3493.4305	65.1084 129.0985 249.8649 750.3085 1042.4585 1200.3334 1397.9887 1498.4617 1659.0028 3091.9437 3160.7880 3610.6055	87.0185 153.0454 344.9326 895.2919 1047.1073 1316.1461 1469.7810 1510.4711 3052.9636 3133.5634 3261.0796 3629.1113
PC2	7.40900 3.46584 2.62493	49.5905 123.5631 173.4903 449.5450 948.8380 1152.7354 1413.7638 1483.6696	97.1527 134.2506 244.5497 901.2400 1039.8468 1187.8084 1418.9539 1486.5006	115.8675 168.8550 364.7199 940.4638 1052.2564 1365.2722 1476.3454 1499.1639

		1656.0422	1660.5253	2994.6838
		2996.6024	3067.2977	3068.6950
		3125.9927	3129.1980	3195.6654
		3487.7666	3604.8709	3629.4283
1-C₃H₇	32.85025 9.10849 7.86702	**77.1218**	**253.2809**	374.4779
		452.9075	754.9938	895.9108
		928.4818	1052.5447	1100.7192
		1177.7976	1270.9268	1362.9367
		1409.5054	1469.8416	1473.5952
		1501.9520	1507.7481	2983.6254
		3056.9735	3061.6766	3128.6587
		3137.5955	3167.3716	3268.5067
2-C₃H₇	37.21890 8.46566 7.54135	**106.8468**	**108.4512**	317.9086
		384.2618	902.6035	938.4022
		947.8995	1026.5043	1156.8770
		1183.8507	1367.0428	1413.8615
		1419.0235	1472.6660	1481.5257
		1483.5723	1495.3811	2991.2398
		2993.6600	3057.2343	3058.0611
		3130.6207	3131.7281	3206.5089
TS1	9.23700 3.75964 3.01851	1700.8998i	**90.7524**	111.5513
		130.8962	**251.0703**	**364.4181**
		392.6256	572.3804	685.0960
		790.3463	835.6196	896.9387
		944.6134	970.9582	1089.4705
		1160.3965	1199.9745	1293.0327
		1359.7313	1363.8259	1412.2996
		1445.3056	1461.3538	1484.8245
		1501.9225	1507.3742	1540.5151
		3035.5842	3058.6551	3073.0157
		3092.8680	3124.0694	3135.4964
		3167.1501	3420.8955	3511.8110
TS2	7.59724 4.37096 3.11586	1603.0704i	**33.4307**	112.5074
		159.1708	**208.1610**	**245.7770**
		366.7258	557.1627	651.5642
		757.1098	880.1001	921.1586
		927.6228	955.6652	1130.4310
		1164.9198	1194.2115	1344.4518
		1383.1446	1400.2286	1413.2426
		1440.9451	1485.7519	1489.8440

	1499.5263	1503.5800	1536.0301
	3040.2465	3042.2723	3091.4037
	3099.4362	3108.0627	3129.0775
	3133.1019	3419.8993	3509.7456

[a] Frequency modes in **bold** corresponds to the internal rotations.

Table S2: M06-2X/aug-cc-pVTZ optimized geometries and CCSD(T)/CBS//M06-2X/aug-cc-pVTZ electronic energies corresponding to the stationary points of the $NH_2 + C_3H_8$ potential energy surface.

Species	Cartesian coordinates / Å			Electronic energies (Hartree)
NH₂	7	0.000000000	0.140953000	0.000000000	-55.823356
	1	0.804325000	-0.493334000	0.000000000	
	1	-0.804325000	-0.493337000	0.000000000	
NH₃	7	-0.000002000	0.000006000	-0.112438000	-56.507545
	1	0.756439000	0.558301000	0.262360000	
	1	0.105318000	-0.934239000	0.262345000	
	1	-0.861744000	0.375899000	0.262363000	
C₃H₈	6	1.263476000	-0.260181000	0.000001000	-118.976131
	1	1.296021000	-0.904389000	-0.880048000	
	1	1.296026000	-0.904370000	0.880064000	
	1	2.164018000	0.353087000	-0.000008000	
	6	0.000000000	0.590503000	-0.000004000	
	1	0.000001000	1.245252000	0.873592000	
	1	-0.000001000	1.245239000	-0.873610000	
	6	-1.263476000	-0.260181000	0.000003000	
	1	-1.296023000	-0.904372000	0.880064000	
	1	-2.164018000	0.353087000	-0.000002000	
	1	-1.296023000	-0.904386000	-0.880048000	
PC1	6	-0.308587000	1.207669000	0.015561000	-174.811800
	1	-0.152583000	1.623215000	-0.969777000	
	1	-0.449553000	1.900459000	0.832368000	
	7	2.691349000	-0.362017000	-0.141845000	
	1	3.648748000	-0.068518000	0.006786000	
	1	2.102926000	0.458289000	-0.042638000	
	1	2.450242000	-0.986960000	0.617677000	
	6	-0.645574000	-0.232603000	0.172937000	
	1	-0.030765000	-0.830805000	-0.502804000	
	1	-0.415153000	-0.559858000	1.189090000	
	6	-2.127964000	-0.516316000	-0.116207000	
	1	-2.351221000	-1.576727000	0.001291000	
	1	-2.768294000	0.046903000	0.562337000	
	1	-2.381043000	-0.224378000	-1.135156000	
PC2	6	-0.968310000	-0.034733000	0.535088000	-174.817807
	1	-1.344407000	-0.063742000	1.548553000	
	7	2.316237000	0.107971000	-0.075046000	

	1	2.992264000	0.771603000	0.281902000	
	1	1.497657000	0.157370000	0.523221000	
	1	2.715371000	-0.814913000	0.044440000	
	6	-1.020044000	1.246486000	-0.218343000	
	1	-0.994346000	2.112448000	0.441495000	
	1	-0.182618000	1.316182000	-0.917553000	
	1	-1.936809000	1.320878000	-0.818466000	
	6	-0.794705000	-1.312708000	-0.205453000	
	1	0.016956000	-1.228950000	-0.932861000	
	1	-0.581515000	-2.148026000	0.460453000	
	1	-1.697858000	-1.572912000	-0.773613000	
1-C₃H₇	6	1.291005000	-0.295968000	-0.030803000	-118.301955
	1	1.253682000	-1.323573000	0.301316000	
	1	2.256924000	0.124488000	-0.265278000	
	6	0.079131000	0.559145000	0.047056000	
	1	0.084035000	1.132861000	0.984318000	
	1	0.104775000	1.310207000	-0.746964000	
	6	-1.215614000	-0.243828000	-0.034624000	
	1	-2.089907000	0.400774000	0.045078000	
	1	-1.274210000	-0.783789000	-0.979606000	
	1	-1.262428000	-0.977063000	0.771363000	
2-C₃H₇	6	-0.010621000	0.544145000	0.000000000	-118.306601
	1	0.229394000	1.597427000	0.000000000	
	6	-0.010621000	-0.199334000	1.286317000	
	1	-0.169183000	0.457565000	2.139772000	
	1	-0.789390000	-0.967164000	1.295928000	
	1	0.939462000	-0.725545000	1.450695000	
	6	-0.010621000	-0.199334000	-1.286317000	
	1	-0.789390000	-0.967164000	-1.295928000	
	1	-0.169183000	0.457565000	-2.139772000	
	1	0.939462000	-0.725545000	-1.450695000	
TS1	6	0.124794000	1.103568000	0.291284000	-174.781554
	1	0.405876000	2.072867000	-0.114306000	
	1	0.019340000	1.143431000	1.374625000	
	7	2.186075000	-0.415658000	-0.107336000	
	1	2.036895000	-1.038678000	0.690190000	
	1	1.187991000	0.429254000	0.110039000	
	1	1.782206000	-0.927313000	-0.896131000	
	6	-1.027558000	0.430991000	-0.412696000	
	1	-1.906477000	1.081729000	-0.363146000	
	1	-0.795278000	0.322323000	-1.474601000	
	6	-1.373479000	-0.926499000	0.186524000	
	1	-2.217901000	-1.386408000	-0.324990000	
	1	-0.525313000	-1.609130000	0.117467000	
	1	-1.632407000	-0.826832000	1.241535000	
TS2	6	0.411455000	0.005075000	0.479369000	-174.784657
	1	0.538265000	0.011693000	1.562000000	
	7	-2.145268000	-0.057222000	0.042811000	
	1	-2.204693000	0.885198000	-0.351374000	

	1	-0.836492000	-0.030961000	0.382209000	
	1	-2.059851000	-0.659754000	-0.779952000	
	6	0.923935000	-1.263967000	-0.157777000	
	1	0.484115000	-2.149294000	0.299931000	
	1	0.695355000	-1.280444000	-1.225134000	
	1	2.010169000	-1.338545000	-0.056117000	
	6	0.887363000	1.281340000	-0.171380000	
	1	0.642673000	1.287480000	-1.235100000	
	1	0.437630000	2.161087000	0.287996000	
	1	1.973184000	1.379402000	-0.085402000	

Table S3: High-pressure rate constant, $k_{TST}(T)$, of $NH_2 + C_3H_8$ reaction, including HIR and Eckart tunneling corrections. Units are in cm^3/molecule/s.

T (K)	k_{TST} (T), cm^3/molecule/s		
	via TS1	via TS2	k_tot
300	1.65E-18	2.72E-17	2.89E-17
400	2.93E-17	2.67E-16	2.96E-16
500	2.68E-16	1.52E-15	1.79E-15
600	1.45E-15	5.71E-15	7.16E-15
700	5.46E-15	1.63E-14	2.18E-14
800	1.59E-14	3.83E-14	5.42E-14
900	3.87E-14	7.82E-14	1.17E-13
1000	8.20E-14	1.44E-13	2.26E-13
1100	1.57E-13	2.44E-13	4.01E-13
1200	2.76E-13	3.89E-13	6.65E-13
1300	4.55E-13	5.88E-13	1.04E-12
1400	7.12E-13	8.52E-13	1.56E-12
1500	1.06E-12	1.19E-12	2.25E-12
1600	1.53E-12	1.62E-12	3.15E-12
1700	2.14E-12	2.15E-12	4.29E-12
1800	2.90E-12	2.78E-12	5.68E-12
1900	3.85E-12	3.54E-12	7.39E-12
2000	5.00E-12	4.43E-12	9.43E-12

+ $k_{\_NH3+N-C3H7}(T) = 2.19\times10^{-26}\times T^{4.52}\times\exp(-2346.7\ K/T)$ (T = 300 – 2000 K, cm^3/molecule/s and fitting error ~ 2.3 %, via TS1)
+ $k_{\_NH3+I-C3H7}(T) = 1.35\times10^{-24}\times T^{3.91}\times\exp(-1684.0\ K/T)$ (T = 300 – 2000 K, cm^3/molecule/s and fitting error ~ 1.5 %, via TS2)
+ $k_{\_tot}(T) = 4.00\times10^{-26}\times T^{4.47}\times\exp(-1566.5\ K/T)$ (T = 300 – 2000 K, cm^3/molecule/s and fitting error ~ 1.6 %)

Table S4: The calculated Eckart tunneling factor for the reactions of $NH_2 + C_3H_8$ over the wide temperature range of 300 – 2000 K.

T (K)	via TS1	via TS2
300	36.80	18.50
400	6.17	4.64
500	3.05	2.61
600	2.14	1.94
700	1.75	1.63
800	1.54	1.46
900	1.41	1.35
1000	1.32	1.28
1100	1.27	1.23
1200	1.22	1.19
1300	1.19	1.17
1400	1.16	1.14
1500	1.14	1.13
1600	1.13	1.11
1700	1.11	1.10
1800	1.10	1.09
1900	1.09	1.08
2000	1.08	1.07

Table S5: The calculated rate constants with and without HIR corrections for the reactions of $NH_2 + C_3H_8$ over the wide temperature range of 300 – 2000 K.

T (K)	k_{tot} (with HIR) [cm³/molecule/s]	k_{tot} (without HIR) [cm³/molecule/s]	HIR factor (k_with_HIR/k_without_HIR)
300	2.89E-17	1.82E-17	1.59
400	2.96E-16	2.05E-16	1.44
500	1.79E-15	1.34E-15	1.34
600	7.16E-15	5.70E-15	1.26
700	2.18E-14	1.83E-14	1.19
800	5.42E-14	4.75E-14	1.14
900	1.17E-13	1.06E-13	1.10
1000	2.26E-13	2.13E-13	1.06
1100	4.01E-13	3.89E-13	1.03
1200	6.65E-13	6.64E-13	1.00
1300	1.04E-12	1.07E-12	0.98
1400	1.56E-12	1.64E-12	0.95
1500	2.25E-12	2.43E-12	0.93
1600	3.15E-12	3.46E-12	0.91
1700	4.29E-12	4.81E-12	0.89
1800	5.68E-12	6.51E-12	0.87
1900	7.39E-12	8.62E-12	0.86
2000	9.43E-12	1.12E-11	0.84

Species	Potential energy surfaces for the internal rotations
C_3H_8	

Species	Potential energy surfaces for the internal rotations
TS1	
TS2	
1-C₃H₇	

| Species	Potential energy surfaces for the internal rotations

2-C₃H₇
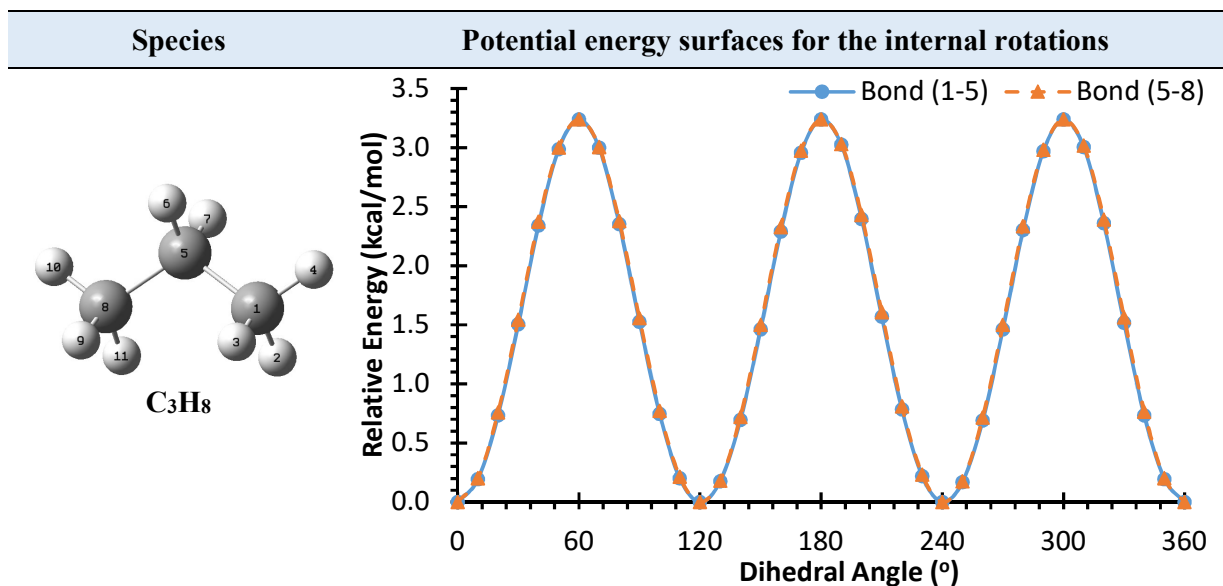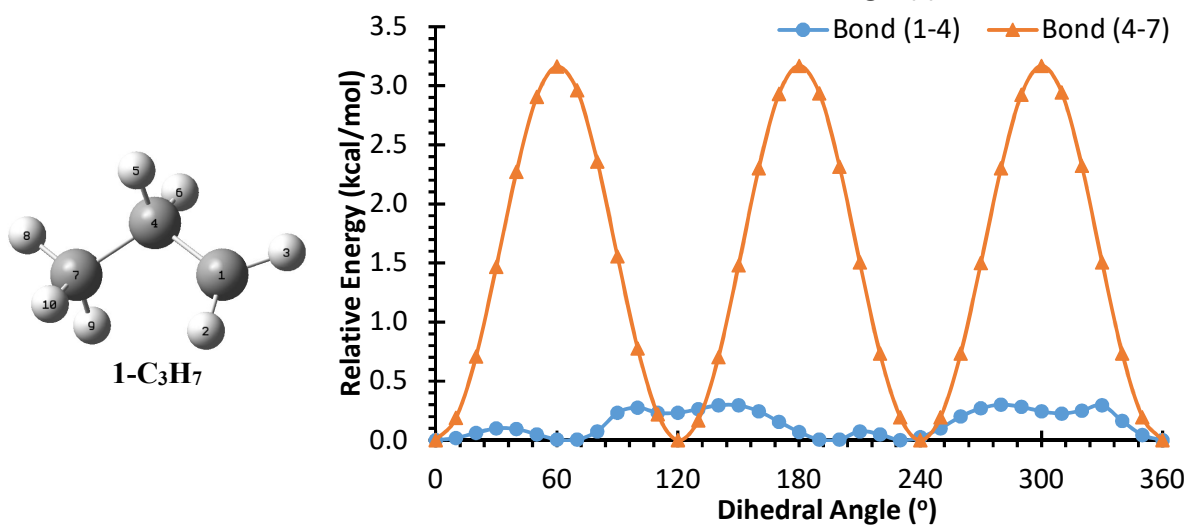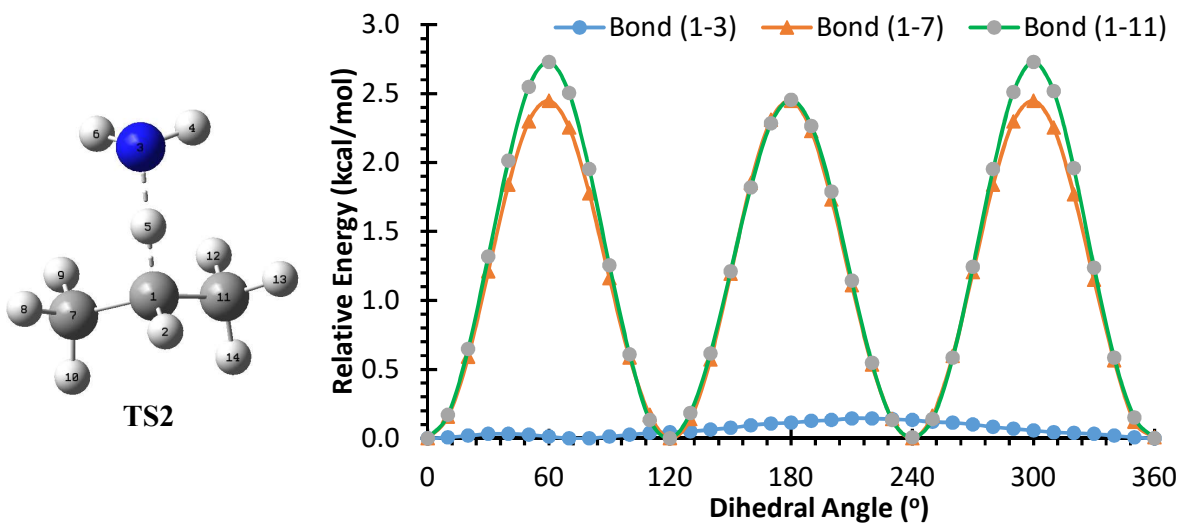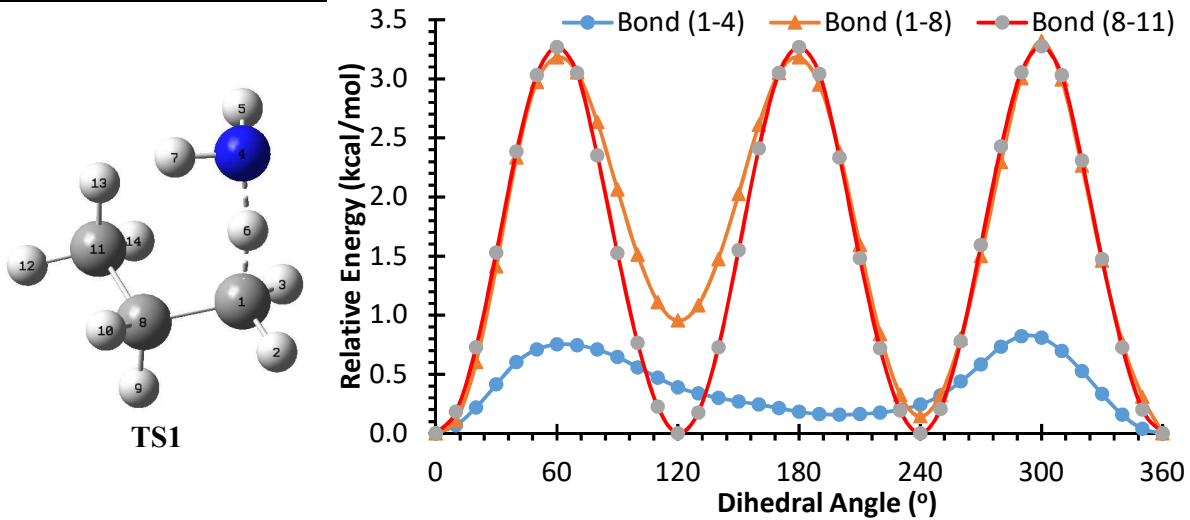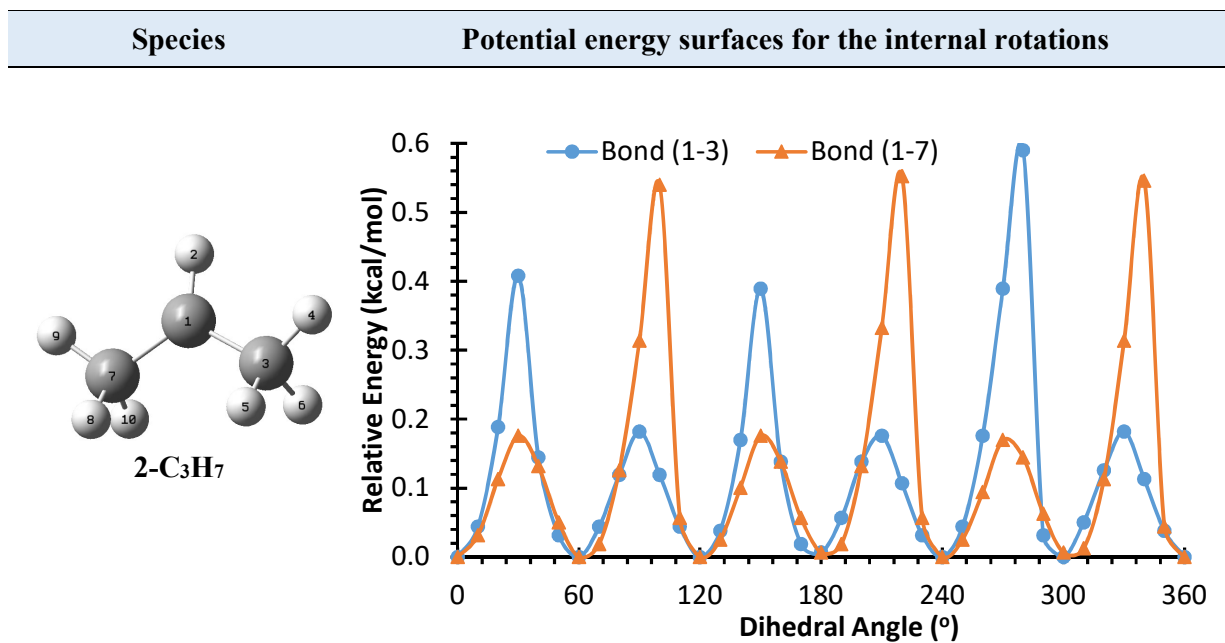
Figure S1: Hindrance potentials for the species involved in the $NH_2 + C_3H_8$ reaction, calculated at M06-2X/cc-pVDZ level of theory.
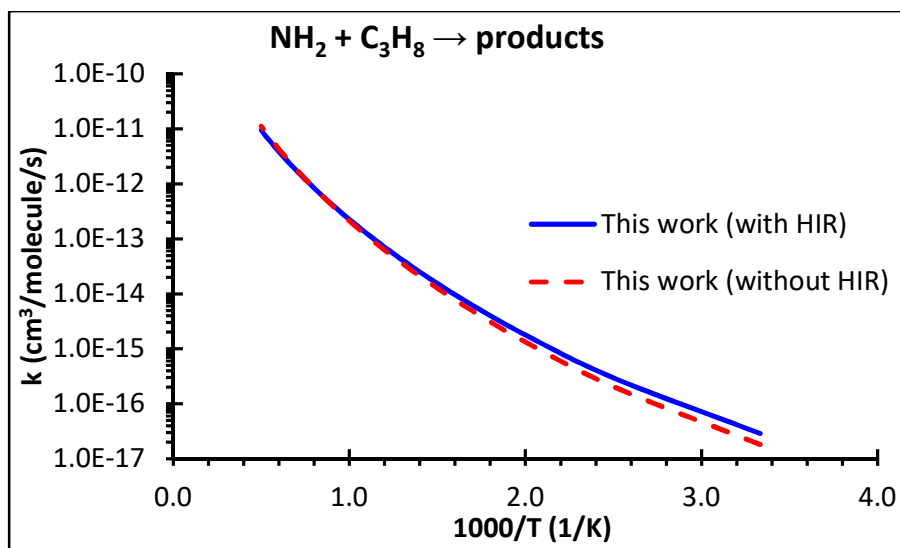
Figure S2: Predicted total rate constant for the reaction of $NH_2 + C_3H_8 \rightarrow$ products, with (solid line) and without (dashed line) HIR treatment.
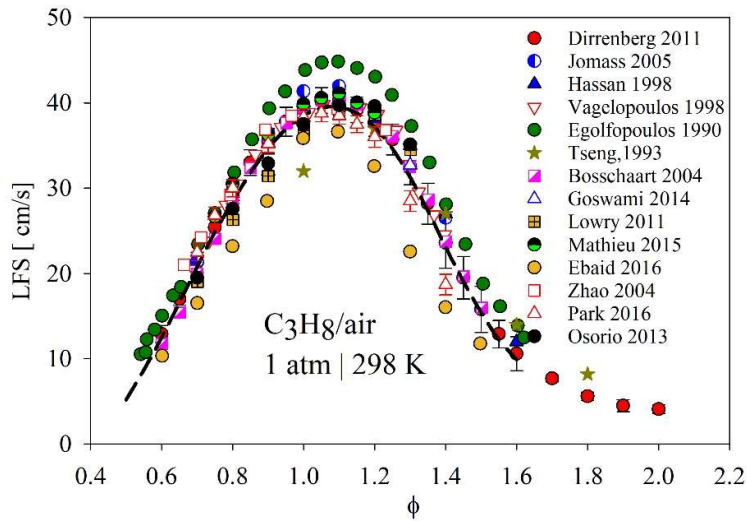
Figure S3: Laminar flame speed of C_3H_8/air at 1 atm and 298 K as a function of equivalence ratio. Symbols: experimental data from literature [2,3,12–14,4–11]. Line: model predictions from this work.
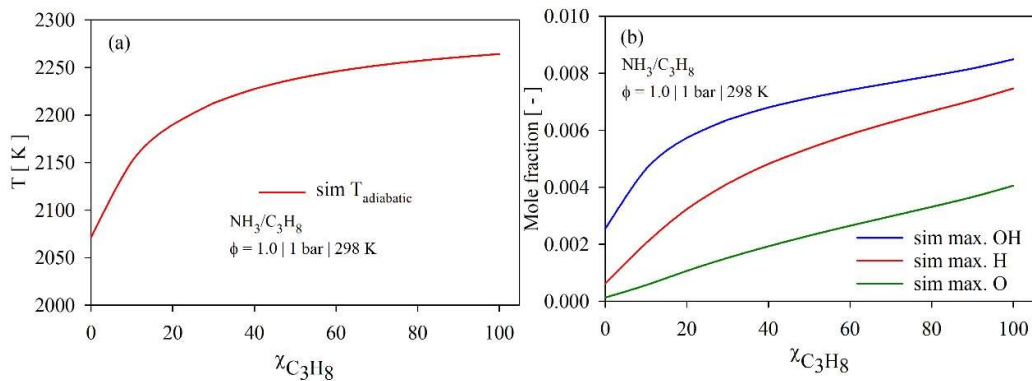

Figure S4: Model predicted adiabatic flame temperature (a) and maximum mole fraction of OH, H and O (b) at ϕ = 1.0, 1 bar and 298 K as a function of C_3H_8 mole fraction variation in the NH_3/C_3H_8 blends for the flame condition shown in Fig. 5b in manuscript.
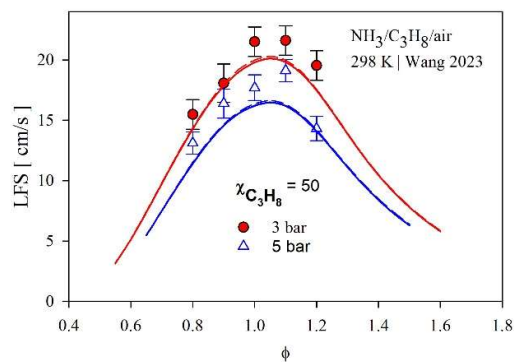
Figure S5: Laminar flame speed of NH_3 50% /C_3H_8 50 %/air at 3 and 5 bar at 298 K. Symbols: experimental data from literature [15]. Lines: model predictions from this work.
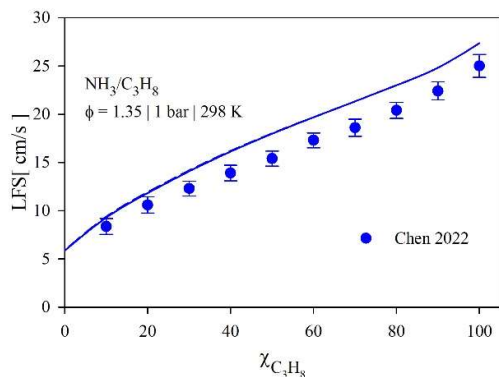

Figure S6: Laminar flame speed of NH_3/C_3H_8/air at varying C_3H_8 content in fuel blend at ϕ = 1.35, 1 bar and 298 K. Symbols: experimental data from literature [16]. Lines: Lines: model predictions from this work.
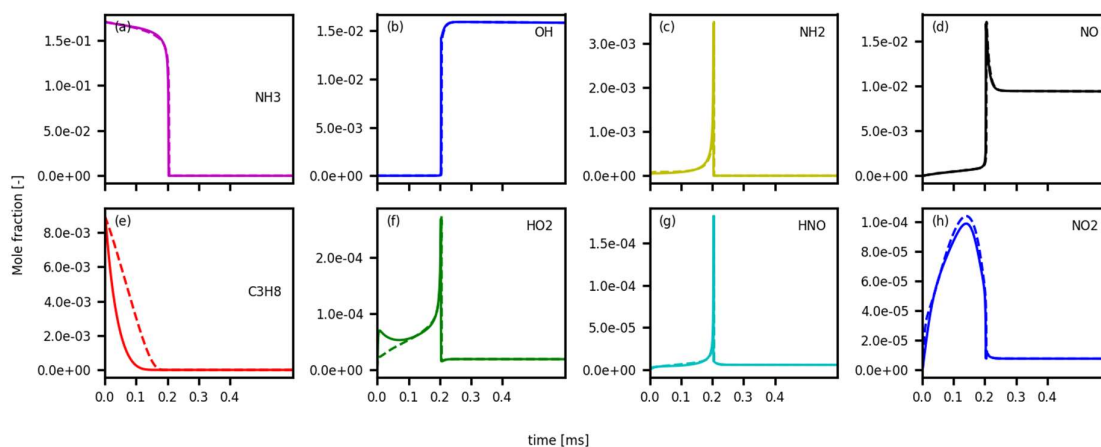

Figure S7: Main species profiles with and without the cross-reaction added in this study at 1400 K, 40 bar and ϕ = 1.0 for 95% NH_3/5%C_3H_8 /air blend. Solid lines: with cross-reactions, dashed lines: without cross-reactions.
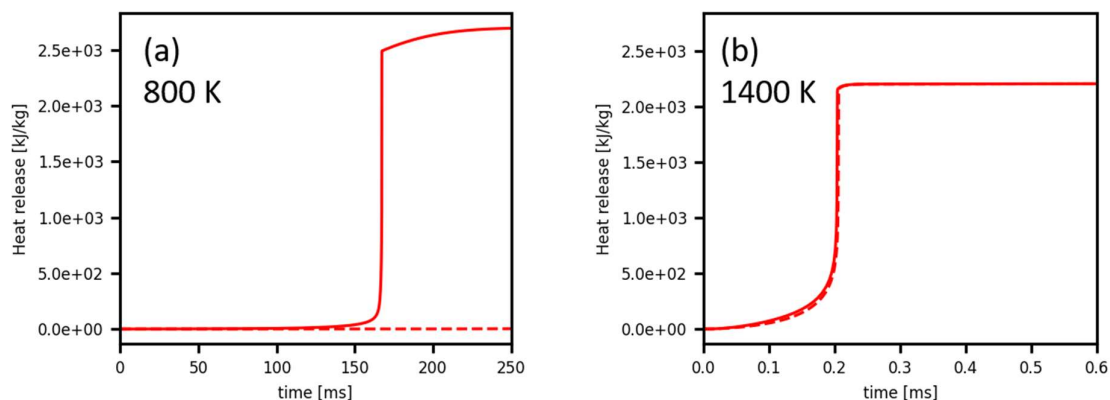
Figure S8: Heat release rate as a function of time at 800 K (a) and 1400 K (b), 40 bar and ϕ = 1.0 for 95% NH$_3$/5%C$_3$H$_8$ /air blend. Solid lines: with cross-reactions, dashed lines: without cross-reactions.

References

[1]   A.M. Mebel, Prediction of absolute rate constants for the reactions of NH2 with alkanes from ab initio G2M/TST calculations, *J. Phys. Chem. A*. 103 (1999) 2088–2096.

[2]   G. Jomaas, X.L. Zheng, D.L. Zhu, C.K. Law, Experimental determination of counterflow ignition temperatures and laminar flame speeds of C2 - C3 hydrocarbons at atmospheric and elevated pressures, *Proc. Combust. Inst.* 30 (2005) 193–200.

[3]   M.I. Hassan, K.T. Aung, G.M. Faeth, Measured and predicted properties of laminar premixed methane/air flames at various pressures, *Combust. Flame*. 115 (1998) 539–550.

[4]   L.-K. Tseng, M.A. Ismail, G.M. Faeth, Laminar Burning Velocities and Markstein Numbers of Hydrocarbon/Air Flames, *Combust. Flame*. 95 (1993) 410–426.

[5]   K.J. Bosschaart, L.P.H. De Goey, The laminar burning velocity of flames propagating in mixtures of hydrocarbons and air measured with the heat flux method, *Combust. Flame*. 136 (2004) 261–269.

[6]   M. Goswami, Laminar Burning Velocities at Elevated Pressures using the Heat Flux Method, Eindhoven University of Technology, 2014.

[7]   W. Lowry, J. de Vries, M. Krejci, E. Petersen, Z. Serinyel, W. Metcalfe, H. Curran, G. Bourque, Laminar Flame Speed Measurements and Modeling of Pure Alkanes and Alkane Blends at Elevated Pressures, *J. Eng. Gas Turbines Power*. 133 (2011) 91501.

[8]   M.S.Y. Ebaid, K.J.M. Al-Khishali, Measurements of the laminar burning velocity for propane: Air mixtures, *Adv. Mech. Eng.* 8 (2016) 1–17.

[9]   O. Park, P.S. Veloo, D.A. Sheen, Y. Tao, F.N. Egolfopoulos, H. Wang, Chemical kinetic model uncertainty minimization through laminar flame speed measurements, *Combust. Flame*. 172 (2016) 136–152.

[10]   C.H. Osorio, A.J. Vissotski, E.L. Petersen, M.S. Mannan, Effect of CF3Br on C1-C3ignition and laminar flame speed: Numerical and experimental evaluation, *Combust. Flame*. 160 (2013) 1044–1059.

[11]   C.M. Vagelopoulos, F.N. Egolfopoulos, Direct experimental determination of laminar flame speeds, *Symp. Combust.* 27 (1998) 513–519.

[12]   F.N. Egolfopoulos, D.L. Zhu, C.K. Law, Experimental and numerical determination of laminar flame speeds: Mixtures of C2 hydrocarbons with oxygen and nitrogen, *Symp. Combust.* 23 (1990) 471–478.

[13]   P. Dirrenberger, H. Le Gall, R. Bounaceur, O. Herbinet, P.A. Glaude, A. Konnov, F. Battin-Leclerc, Measurements of laminar flame velocity for components of natural gas, *Energy and Fuels*. 25 (2011) 3875–3884.

[14]   Z. Zhao, A. Kazakov, J. Li, F.L. Dryer, The initial temperature and N2dilution effect on the laminar flame speed of propane/air, *Combust. Sci. Technol.* 176 (2004) 1705–1723.

[15]   Z. Wang, C. Ji, D. Wang, T. Zhang, Y. Zhai, S. Wang, Experimental and numerical study on laminar burning velocity and premixed combustion characteristics of NH3/C3H8/air mixtures, *Fuel*. 331 (2023) 125936.

[16]   C. Chen, Z. Wang, Z. Yu, X. Han, Y. He, Y. Zhu, A.A. Konnov, Experimental and kinetic modeling study of laminar burning velocity enhancement by ozone additive in NH3+O2+N2 and NH3+CH4/C2H6/C3H8+air flames, *Proc. Combust. Inst.* (2022).